Equation-of-State Measurement of Dense Plasmas Heated With Fast Protons

G. M. Dyer,[1] A. C. Bernstein,[1] B. I. Cho,[1] J. Osterholz,[1] W. Grigsby,[1] A. Dalton,[1] R. Shepherd,[2] Y. Ping,[2] H. Chen,[2] K. Widmann,[2] and T. Ditmire[1]

[1]*Texas Center for High Intensity Laser Science, Department of Physics, The University of Texas at Austin, Austin, Texas 78712, USA*
[2]*Lawrence Livermore National Laboratory, Livermore, California 94550, USA*

(Received 18 May 2007; published 2 July 2008)

Using an ultrafast pulse of mega-electron-volt energy protons accelerated from a laser-irradiated foil, we have heated solid density aluminum plasmas to temperatures in excess of 15 eV. By measuring the temperature and the expansion rate of the heated Al plasma simultaneously and with picosecond time resolution we have found the predictions of the SESAME Livermore equation-of-state (LEOS) tables to be accurate to within 18%, in this dense plasma regime, where there have been few previous experimental measurements.

DOI: 10.1103/PhysRevLett.101.015002 PACS numbers: 52.25.Kn, 52.27.Gr, 52.38.Ph, 52.50.Gj

The study of the properties of matter at the convergence of condensed matter and plasma physics, often termed warm dense matter (WDM), is an active and growing field of research. Understanding and characterizing this exotic regime is important to modeling many phenomena found in astrophysics [1], inertial confinement fusion [2], and geophysics [3]. These states of matter, associated with temperatures of $\sim$1–100 eV and $\sim$0.1–10 times solid density, are ionized, like traditional plasmas, but differ from the traditional descriptions of condensed matter and plasma physics because the thermal energy is near or above the Fermi energy and the ion-ion strong coupling parameter [4] is near or above unity. Developing physical models of these strongly coupled plasmas, in which quantum effects are often important, is difficult: standard plasma kinetic theory, usually based on uncorrelated two-body interactions, breaks down and degeneracy effects may become important. This difficulty is evident in the constructions of some early SESAME equation-of-state (EOS) tables [5,6], which were formulated in the warm-dense region from a patchwork of interpolations between established theories. To avoid the thermodynamic inconsistencies arising from interpolations, a global EOS with adjustable parameters, such as the widely used Thomas-Fermi-based quotidian equation of state (QEOS) [7], is often preferred. Such models ignore some of the physics of WDM, and can be inaccurate where empirical data are lacking. Recently, creative new theoretical approaches have been developed to model WDM properties (e.g., [8,9]). However, their validation still requires experimental measurements on well-characterized dense plasma states.

WDM conditions can be accessed in a number of ways, such as static compression accompanied by laser heating [10], strong shocks [3,11], and heating with ultrafast laser or other radiation pulses [12–14]. Because the plasma is only inertially confined in the latter approach, effective heating must be completed before the sample has a chance to expand appreciably, a time scale roughly given by d/c_s if d is the heated sample thickness and c_s is the heated sample sound speed. For micron thickness samples, this requires heating on a picosecond time scale for the megabar pressures of WDM. Intense femtosecond lasers are a natural choice for ultrafast heating [13,15], but the standard laser wavelengths in and near the visible are limited to a short penetration depth of $<$100 nm. Uniform, isochoric heating utilizing lasers in the visible wavelength region requires ultrathin (20–30 nm), freestanding targets and existing oxide layers and surface contamination start to have a significant impact on the hydrodynamic behavior [13]. Furthermore, the sample must be optically thick if brightness temperature is to be used as a temperature measurement [16].

Recent developments in laser and pulsed power technology make access to WDM states possible by enabling the generation of ultrafast pulses of secondary radiation, such as x rays, electrons or fast protons, which are more penetrating at solid density than optical photons. One promising source for volumetric heating is an intense laser driven proton beam. High energy proton pulses are produced when a laser pulse at intensity $>10^{18}$ W/cm^2 is incident upon a thin foil. Hot electrons generated on the front foil surface traverse the foil and exit the back, building up a virtual cathode. This accelerates hydrogen ions from contaminant layers on the surface to multi-mega-electron-volt energies [17]. This approach has higher conversion efficiency into heating of a sample than laser-generated hot electrons or x rays [18]. Previously it was shown by Patel *et al.* [12] and Antici *et al.* [19] that these laser-generated protons could heat solid density matter isochorically to temperatures up to 20 eV.

In this Letter we report on experiments in which we investigated the EOS of Al by applying isochoric proton heating on a well-characterized Al sample, and simultaneously measured time histories of the target expansion and temperature. We heated the target with an ultrafast pulse of protons to temperatures of 20 eV while maintain-

ing densities near that of the cold material. Pressure information was obtained from chirped-pulse interferometry (CPI) [20], which measured the 1D target expansion into vacuum [16]. Temperature was determined from the high-frequency visible region of the thermal emission spectrum with a streaked optical pyrometer (SOP) [12,19,21], which incorporated an absolutely calibrated ultrafast streak camera. In conjunction with hydrodynamic simulations the simultaneous measurement of temperature and expansion rate allows us to evaluate two equation-of-state tables for near solid density Al: the Livermore equation-of-state (LEOS) tables, generated using QEOS, and the SESAME 3718 table [22], at temperatures up to 20 eV.

We performed our experiment at the Titan laser in the Jupiter Laser Facility at Lawrence Livermore National Laboratory [23]. Laser pulses of 1 μm wavelength with 100 J of energy in a 500 fs pulse were focused to a <10 μm focal spot on a flat source foil of 17 μm Al to generate mega-electron-volt protons (Fig. 1). The laser-generated proton beam traversed a 400 μm vacuum gap to heat a sample foil of 2 μm Al supported on 500 nm Au and 25 nm SiN_3. The protons were diagnosed with a proton spectrometer placed normal to the source foil surface. To produce the chirped pulse of 130 ps for the CPI diagnostic, a 5 mJ probe beam was extracted from an early stage of the laser chain and only partially recompressed. The CPI probe was incident with S polarization on the sample back surface at 15° from normal, timed to cover the period of proton heating. The reflected probe was imaged into a Mach-Zehnder interferometer and relay imaged onto the slit of a high-resolution spectrometer [20]. For the SOP diagnostic we imaged the heated region of the sample with $f/3.1$ optics through a 10 nm bandwidth interference filter centered at a wavelength of 470 nm (chosen to be away from harmonics of the pump) and onto the slit of a Hamamatsu C7700 streak camera (3 ps temporal resolution). The magnification, time scale, optics throughput, and streak camera response were calibrated to allow direct measurement of the brightness temperature.

An example of SOP raw data is shown in Fig. 2(a) showing thermal emission from the heated target as a function of time. The brightest part of the image corresponds to proton heating, but we see an initial pulse of light in advance of the main heating. If this initial pulse is taken to start at $t = 0$, the onset of the heating is consistent with

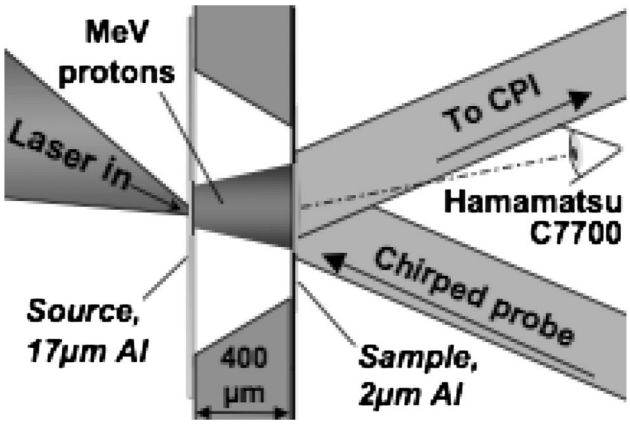

FIG. 1. A two foil, vacuum spaced target for proton heating. A 100 J, 500 fs pump laser is focused to a 10 μm spot from the left onto the 17 μm source foil. Protons generated from the source back surface traverse the 400 μm vacuum gap, heating the 2 μm Al sample layer. The support frame was etched from a Si wafer. The mirror finish of the Al sample allows clean reflection from the back surface. The probe reflected at 15° from normal, while the SOP imaged the sample surface at 15° above the plane, allowing the proton spectrum to be measured from the normal direction.

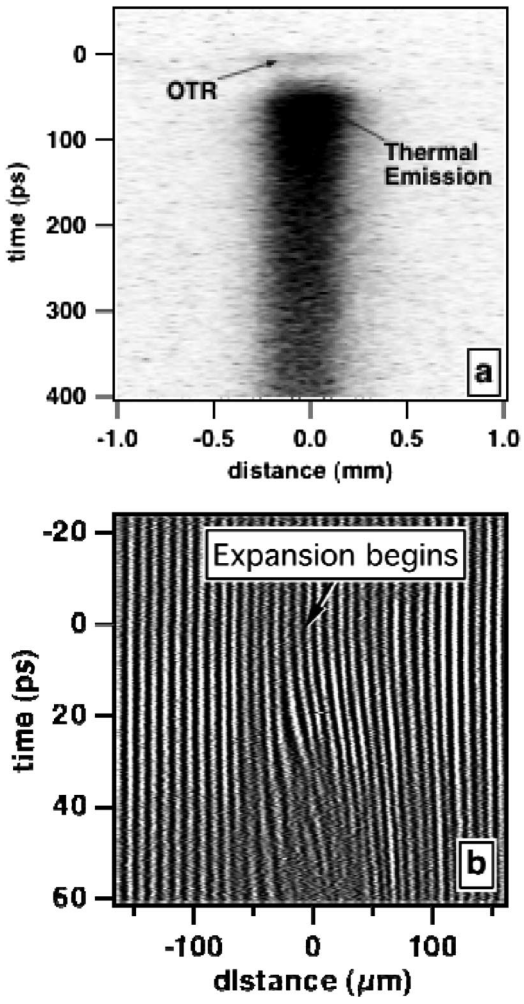

FIG. 2. Raw images from our two time-resolved diagnostics. (a) An SOP image, showing both OTR and thermal emission. The OTR is offset 200 μm spatially from the proton heating center, consistent with a target-normal trajectory for the protons and electrons traveling in the laser direction. (b) A raw CPI image, showing a disturbance that starts in the middle of the time window viewed. This image is Fourier analyzed along horizontal lineouts to extract phase and reflectivity.

the proton transit time across the 400 μm vacuum gap, calculated from the measured proton energy distribution as discussed below. The initial pulse is then identified with optical transition radiation (OTR) [24], first from electrons traveling at approximately the speed of light in the laser direction, and then by the fastest protons, both of which pass through the sample without depositing appreciable energy. The spatial and temporal shape and the brightness of the initial pulse are consistent with this interpretation. The actual heating is seen to take place between 10 and 50 ps after the OTR, with a peak brightness temperature of >15 eV (see Fig. 3), followed by a slow cooling. The rate

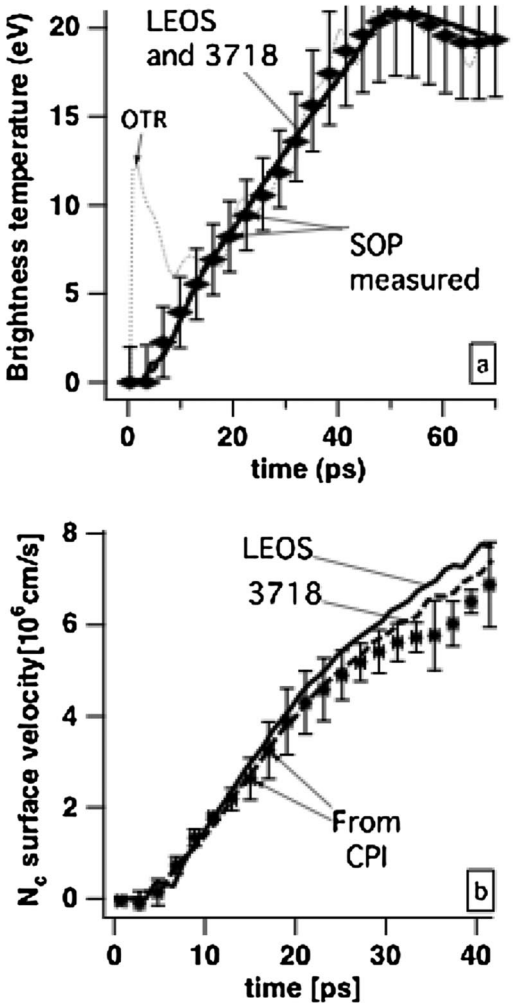

FIG. 3. Comparison of SOP and CPI data from the same shot using HYADES simulations with SESAME EOS 3718 (solid curves) and LEOS (dashed curves) models. (a) A lineout of the SOP measured brightness temperature, with OTR removed, and the simulated signal achieved using a rough fit to the proton spectrum as an energy input to HYADES, scaled to best fit the SOP data for the two EOS models. The simulation curves overlap here and continue to match the SOP data beyond 100 ps. (b) Points show lineout of expansion velocity measured by the CPI on the same shot; lines show calculated expansion from the simulations.

of heating matches well with what is predicted from an independent measurement of the proton spectrum.

Raw data from the CPI measurement of the target expansion are illustrated in Fig. 2(b). Here the onset of heating, marked by a deviation in fringe position, occurs during the probe pulse interaction: straight fringes are continuously bent as the target expands. We applied a Fourier reconstruction procedure along lineouts of these data to account for the effects of Doppler shifting within the probe beam [20]. The time scale of the CPI is determined by the chirp of the probe beam, which was found from the compressor grating configuration relative to that of full compression. This time scale was verified using test shots at various known delays.

Our measurement indicated that the expansion rate of the critical density surface approached 5×10^4 m/s at a temperature of 20 eV. This temperature corresponds to an ion-ion coupling parameter [4] of $\Gamma \approx 100$ at the center of the foil thickness, and $\Gamma \approx 10$ at the critical density surface. To compare our data with the EOS tables, we simulated the expanding foil with the 1D Lagrangian radiative hydrodynamics code HYADES [25]. The code assumed local thermal equilibrium, but allowed for different ion and electron temperatures. Data from the CPI and SOP were compared using lineouts through the spatial regions of highest temperatures and fastest expansion, which were of large enough spatial extent ($\sim$300 μm) relative to that of the maximum measured expansion (1 μm) to justify using a 1D geometry. For each EOS, we simulated a 2 μm planar slab of aluminum on 500 nm of gold. In order to compare the simulation with the brightness temperature measurements of the SOP, at each time step of the simulation we found the temperature at the critical density layer of the SOP wavelength and viewing angle, and multiplied the Planck function at that temperature by the emissivity, calculated from the wave equation in the expanding plasma [26]. We simulated proton heating with a time-dependent energy source into the target electrons, which was constructed from an approximate fit to the measured proton spectrum using the sum of three Maxwellians ($kT =$ 20 MeV, 2 MeV, and 200 keV) and scaled to minimize the error-weighted χ^2 error between the simulated and measured brightness temperatures during heating. With the brightness temperature matched in this way, we then calculated the expansion of the critical density layer at the CPI wavelength and incidence angle, taking into account the (small) phase correction effect of the leading underdense plasma. The result of this analysis is shown in Fig. 3.

Figure 3(a) illustrates the brightness temperature in the hottest, central region as a function of time, with simulations using various EOS models and the criteria described above. Figure 3(b) illustrates the associated expansion rates compared to the measurement of the CPI. We see that, when the input energy is scaled such that the simulated brightness temperature best fits the SOP data, as in

Fig. 3, the simulation using SESAME 3718 matches the expansion velocity more closely than the simulation using LEOS, which falls outside of the error bars at later times. We therefore conclude that our data strongly suggest that SESAME 3718 is the more accurate EOS for near sold density Al in this temperature regime. This is not surprising, as SESAME 3718 uses a more sophisticated model than LEOS. However, it should be noted that we were also able to run simulations with LEOS for which the simulated brightness temperature curve remains within the SOP error bars (on the colder side) and at the same time the simulated velocity curve stays within the error of the CPI measurement. Thus, because of the size of the error bars in the SOP measurement, we cannot categorically reject the accuracy of the LEOS tables.

The balance of free electrons (Z_{eff}) is important in determining critical density surfaces of reflection and self-emission, as well as the surface emissivity and the (small) phase shift from the leading low-density plasma. The LEOS tables included data specifying Z_{eff} across our range of temperatures and densities, ensuring consistency with the EOS. The SESAME 3718 tables provided with HYADES did not have accompanying Z_{eff} tables, and so an internal Thomas-Fermi-based model was used instead. Although the values obtained in this way are expected to be very close, the Z_{eff} values could not be assumed to be perfectly consistent with SESAME 3718. We have conducted other simulations using this approach with the LEOS EOS and have found that using the internal Thomas-Fermi ionization model in HYADES does not significantly affect the simulated expansion velocity.

The NIST proton stopping power tables are not expected to be valid for ionized matter and true stopping powers are expected to depend on ionization level and density [27]. Together with a more thorough proton measurement, more accurate stopping rates would improve this experiment by further constraining the simulation. However, WDM proton stopping power data is lacking, and so we allowed deviations from our proton spectrum, particularly at later times ($>$40 ps), in order to fit the SOP more closely. Another concern is the nonuniformity of heating in the target-normal direction caused by stronger absorption in the Au layer and heating by comoving electrons [28]. These effects were taken into account and found to have negligible effect on our measurements on the time scale observed, during which the back side of the Al foil remains uniformly heated. Radiative heat transfer was handled simply with a gray model [25] and opacities from SESAME tables. We found from simulations that the effects of radiation transfer were negligible on the time scales shown in Fig. 3.

In conclusion, we have measured the expansion and brightness temperature of a foil heated by an ultrafast, laser-generated proton source, using two independent and simultaneous time-resolved diagnostics. We ran hydrodynamic simulations of the foil using energy input derived from the measured proton spectrum and scaled to reproduce the measured temperature history, and compared the resulting simulated expansion to the measured expansion. The LEOS tables are shown to be accurate in this temperature range, within the measurement error of the diagnostics. Greater detail about our diagnostics and analysis will be presented in a future publication. Future experiments will focus on making the heating more instantaneous, both by thickening the sample foil and by decreasing the vacuum gap between source and sample, and on reducing the overall measurement error of the diagnostics.

We would like to acknowledge helpful conversations with Andrew Ng, Pravesh Patel, Jon Larson, and Patrick Audebert. This work was supported by a contract from V-Division at Lawrence Livermore National Laboratory and by the National Nuclear Security Administration under Cooperative agreement No. DE-FC52-03NA00156.

[1] T. Guillot, Science **286**, 72 (1999).
[2] M. Koenig *et al.*, Appl. Phys. Lett. **72**, 1033 (1998).
[3] G. Huser *et al.*, Phys. Plasmas **12**, 060701 (2005).
[4] S. Ichimaru, Rev. Mod. Phys. **54**, 1017 (1982).
[5] K. S. Trainor, J. Appl. Phys. **54**, 2372 (1983).
[6] K. S. Holian, LANL Technical Report No. LA-10160-MS, UC-34,, 1984.
[7] D. A. Young and E. M. Corey, Appl. Phys. **78**, 3748 (1995).
[8] D. Beule *et al.*, Phys. Rev. E **63**, 060202(R) (2001).
[9] J. Clerouin and S. Mazevet, J. Phys. IV **133**, 1071 (2006).
[10] D. Errandonea, J. Phys. Chem. Solids **67**, 2017 (2006).
[11] M. D. Knudson *et al.*, Phys. Rev. B **69**, 144209 (2004).
[12] P. K. Patel *et al.*, Phys. Rev. Lett. **91**, 125004 (2003).
[13] K. Widmann *et al.*, Phys. Plasmas **8**, 3869 (2001).
[14] R. W. Lee *et al.*, AIP Conf. Proc. **581**, 45 (2001).
[15] T. Ao *et al.*, Phys. Rev. Lett. **96**, 055001 (2006).
[16] A. Ng *et al.*, Laser Part. Beams **23**, 527 (2005).
[17] M. Allen *et al.*, Phys. Rev. Lett. **93**, 265004 (2004).
[18] G. Dyer *et al.*, J. Mod. Opt. **50**, 2495 (2003).
[19] P. Antici *et al.*, J. Phys. IV **133**, 1077 (2006).
[20] J. P. Geindre, P. Audebert, S. Rebibo, and J. C. Gauthier, Opt. Lett. **26**, 1612 (2001).
[21] P. Celliers and A. Ng, Phys. Rev. E **47**, 3547 (1993).
[22] S. Lyon and J. Johnson, LANL Technical Report No. LA-CP-98-100, 1992.
[23] A. Ng, http://www.llnl.gov/str/JanFeb07/Ng.html.
[24] J. J. Santos *et al.*, Phys. Rev. Lett. **89**, 025001 (2002).
[25] J. T. Larsen and S. M. Lane, J. Quant. Spectrosc. Radiat. Transfer **51**, 179 (1994).
[26] H. M. Milchberg and R. R. Freeman, J. Opt. Soc. Am. B **6**, 1351 (1989).
[27] D. O. Gericke, M. Schlanges, and T. Bornath, Phys. Rev. E **65**, 036406 (2002).
[28] E. Brambrink *et al.*, Phys. Rev. E **75**, 065401 (2007).